Fusion Engineering and Design 85 (2010) 1283–1289

Contents lists available at ScienceDirect

Fusion Engineering and Design

journal homepage: www.elsevier.com/locate/fusengdes

The impact of lithium wall coatings on NSTX discharges and the engineering of the Lithium Tokamak eXperiment (LTX)

R. Majeski[a,*], H. Kugel[a], R. Kaita[a], S. Avasarala[a], M.G. Bell[a], R.E. Bell[a], L. Berzak[a], P. Beiersdorfer[b], S.P. Gerhardt[a], E. Granstedt[a], T. Gray[a], C. Jacobson[a], J. Kallman[a], S. Kaye[a], T. Kozub[a], B.P. LeBlanc[a], J. Lepson[b], D.P. Lundberg[a], R. Maingi[c], D. Mansfield[a], S.F. Paul[a], G.V. Pereverzev[d], H. Schneider[a], V. Soukhanovskii[b], T. Strickler[a], D. Stotler[a], J. Timberlake[a], L.E. Zakharov[a], The NSTX and LTX Research Teams

[a] Princeton Plasma Physics Laboratory, PO Box 451, Princeton, NJ 08543, USA
[b] Lawrence Livermore National Laboratory, 7000 East Avenue, Livermore, CA 94550, USA
[c] Oak Ridge National Laboratory, PO Box 2008, Oak Ridge, TN 37831, USA
[d] Max-Planck-Institut Für Plasmaphysik, EURATOM Association, Boltzmanstrasse 2, D-85748 Garching, Germany

ARTICLE INFO

Article history:
Available online 14 April 2010

Keywords:
Lithium
Spherical tokamak
Plasma-facing components

ABSTRACT

Recent experiments on the National Spherical Torus eXperiment (NSTX) have shown the benefits of solid lithium coatings on carbon PFC's to diverted plasma performance, in both L- and H-mode confinement regimes. Better particle control, with decreased inductive flux consumption, and increased electron temperature, ion temperature, energy confinement time, and DD neutron rate were observed. Successive increases in lithium coverage resulted in the complete suppression of ELM activity in H-mode discharges. A liquid lithium divertor (LLD), which will employ the porous molybdenum surface developed for the LTX shell, is being installed on NSTX for the 2010 run period, and will provide comparisons between liquid walls in the Lithium Tokamak eXperiment (LTX) and liquid divertor targets in NSTX.

LTX, which recently began operations at the Princeton Plasma Physics Laboratory, is the world's first confinement experiment with full liquid metal plasma-facing components (PFCs). All materials and construction techniques in LTX are compatible with liquid lithium. LTX employs an inner, heated, stainless steel-faced liner or shell, which will be lithium-coated. In order to ensure that lithium adheres to the shell, it is designed to operate at up to 500–600 °C to promote wetting of the stainless by the lithium, providing the first hot wall in a tokamak to operate at reactor-relevant temperatures. The engineering of LTX will be discussed.

1. Introduction

The National Spherical Torus eXperiment (NSTX) is a low aspect ratio toroidal confinement device, with plasmas typically having a major radius of 0.85 m and minor radius up to 0.65 m. Elongations are in the range of 1.6–2.8 in discharges with either a single or double null divertor configuration. Toroidal magnetic fields are from 0.3 to 0.55 T at the magnetic axis, and plasma currents are typically between 0.6 and 1.5 MA. Auxiliary heating capabilities on NSTX include 7 MW of deuterium neutral beam injection (NBI), and 6 MW of high-harmonic fast-wave (HHFW) power at a frequency of 30 MHz [1,2]. Most of the plasma-facing components (PFCs) in NSTX are carbon tiles.

The effect of lithium coatings on PFCs has been a primary focus of recent NSTX research. Such surfaces are expected to improve plasma performance by reducing recycling and suppressing oxygen impurities. This has been observed in other magnetic confinement devices when PFCs were coated with lithium, including TFTR [3], T-11 [4], FT-U [5] and the stellarator TJ-II [6]. A particularly salient result was achieved in the CDX-U device, where a record enhancement in the confinement time of ohmically-heated plasmas was observed in discharges with a toroidal liquid lithium limiter [7,8].

The follow-on device to the CDX-U liquid lithium limiter experiments is the Lithium Tokamak eXperiment – LTX. The LTX will be somewhat larger than CDX-U (R_0 = 0.4 m, a = 0.26 m, κ = 1.6), but like CDX-U it will operate with a limited, rather than a diverted, discharge. However, LTX is designed to employ a thin-film liquid lithium wall covering 90% of the plasma-facing area (5 m^2), whereas in CDX-U the liquid lithium limiter covered only 5% (0.2 m^2) of the last closed flux surface. In LTX, the maximum plasma current will be

* Corresponding author. Tel.: +1 609 243 3112; fax: +1 609 243 2418.
E-mail address: rmajeski@pppl.gov (R. Majeski).

0920-3796/$ – see front matter © 2010 Elsevier B.V. All rights reserved.
doi:10.1016/j.fusengdes.2010.03.020

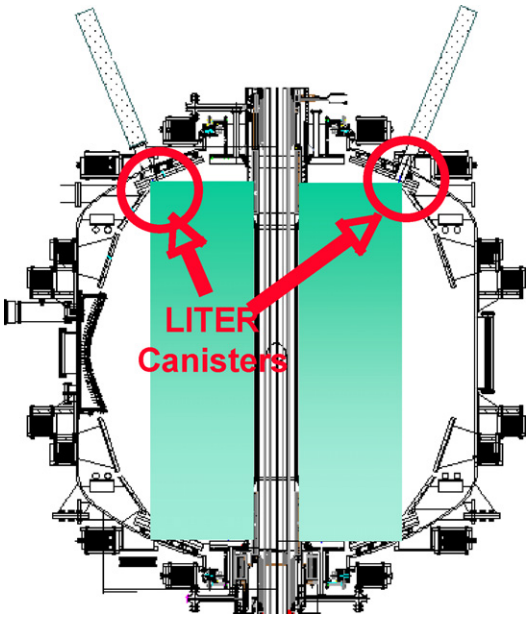

Fig. 1. Elevation of NSTX indicating locations of LiThium EvaporatoRs (LITERs) for coating plasma-facing components in lower region vacuum vessel. Arrows indicate centroid of distribution and shaded regions depict 1/*e* limit of lithium deposition.

increased to 400 kA, with a 50 ms flattop. The toroidal field will also be increased to 3.4 kG. LTX has has begun plasma operation, and is presently scheduled to begin operations with liquid lithium walls early in 2010. The research goal of the LTX program is to produce tokamak discharges with very low global recycling, and determine the consequences for transport and stability of operating in this limit. Many engineering features of LTX have been developed to accommodate the use of liquid lithium as the primary PFC.

2. Lithium coating techniques and their effects in NSTX

The NSTX has two LiThium EvaporatoRs (LITERs), which are lithium ovens mounted on the upper dome of the vacuum vessel (Fig. 1) [9]. They are separated toroidally by about 150°, and have apertures that point downwards to permit lithium deposition on the PFCs in the lower divertor region. Lithium evaporation rates up to about 80 mg/min have been achieved for periods between 5 and 15 min. Since the LITERs cannot be cooled rapidly enough to stop evaporation during discharges, shutters have been installed to interrupt the emission of lithium.

Surface conditioning with lithium coatings has allowed both boronization [10], which used to be conducted after about two weeks of plasma operation, and helium glow-discharge cleaning (HeGDC) between tokamak discharges to be largely discontinued. The effect of the lithium coating, however, appears to be significant for only one or two discharges. Lithium applied after the last discharge on a given day still does improve the performance of the first plasma the next morning. This may mean that it is plasma–surface interactions, and not reactions between the lithium and the residual gas in the vacuum chamber, that determines how active the lithium coating remains.

Modifications to the characteristics of NSTX H-mode plasmas due to lithium coatings have been observed since the beginning of LITER operation. Effects included a lowering in deuterium recycling, and the line emission from the divertor region of low-ionization states of oxygen and carbon decreased. These changes were accompanied by a significant improvement in the energy confinement time with lithium [11]. At the same time, however, the average Z_{eff} and the total power radiated from the plasma both increase. The rise in the Z_{eff} appears to be related to increased carbon impurities in the discharge, while metallic impurities, especially iron, seem to be responsible for the rise in radiated power.

A reduction in the frequency of edge-localized modes (ELMs) was also seen from the earliest use of lithium coatings. In subsequent experiments, an almost complete suppression of ELMs was achieved while maintaining the H-mode [12]. H-mode discharges without lithium-coated PFCs clearly displayed ELMs. These plasmas were analyzed for MHD stability, and had edge plasma characteristics that made them close to the stability boundary for peeling-ballooning modes. When lithium was applied, the edge profiles were modified such that the stability boundary occurred well beyond the range associated with the new experimental equilibria [13].

Recent experiments have explored the cumulative effects of lithium on PFCs. Discharges were programmed to have the same plasma current and NBI power, and as shown in Fig. 2, discharge durations lengthened with increasing lithium. There was also a systematic decrease in the rate of density rise and the deuterium Balmer-alpha emission from the lower divertor region, both attributable to reduced recycling.

The electron density and temperature profiles are compared in Fig. 3 for a discharge without lithium-coated PFCs and a plasma after evaporation of 250 mg of lithium. The measurements were taken near the time of peak plasma stored energy. The electron temperature profile clearly broadens with the application of lithium. In Fig. 4, the stored energies are compared for a set of shots that are similar except for the presence or absence of lithium PFC coatings. The total electron stored energy, calculated by volume integration of the Thomson scattering data, is plotted as a function of the total plasma stored energy, obtained with the EFIT02 code, an equilibrium analysis constrained by external magnetics, electron profile shape, and diamagnetic flux [14]. The 44% increase in electron confinement suggests that the electron channel is primarily responsible for the overall confinement improvement with lithium. The effect of the lithium PFCs on the electron confinement appears to be related to a broadening in the electron temperature profile, rather than an increase in the central temperature. Associated with this is a lower loop voltage and a broader current density profile, as deduced from a lower internal inductance during the current flattop. These have been observed earlier in the liquid lithium experiments in CDX-U [7,8], and the more efficient inductive flux consumption enables longer discharges. Electron thermal diffusivities have been calculated by TRANSP with experimentally-determined parameters, and they indicate a reduction that correlates with improved global electron confinement [15].

A second method for introducing lithium into NSTX has been recently developed. This involves the injection of fine lithium powder (~40 μm particle size) during a discharge into the plasma scrape-off layer. The powder was loaded into a small vacuum chamber connected to a port on top of the NSTX vacuum vessel. A disc of piezo-electric material was oscillated so that the lithium powder fell through a small hole in its center. Preliminary results from the injection lithium powder into the edge of NBI heated deuterium discharges often yielded comparable changes in performance to those with pre-coating the PFCs prior to discharges.

3. Plans for NSTX

The next phase of NSTX lithium research will investigate liquid metal surfaces using a liquid lithium divertor (LLD) (Fig. 5). The LLD is a toroidal conic section with its plasma-facing surface coated with a porous molybdenum layer. Lithium will be evaporated onto the plate, which is heated above the melting point of lithium. The resulting thin liquid layer should have a much larger capacity for

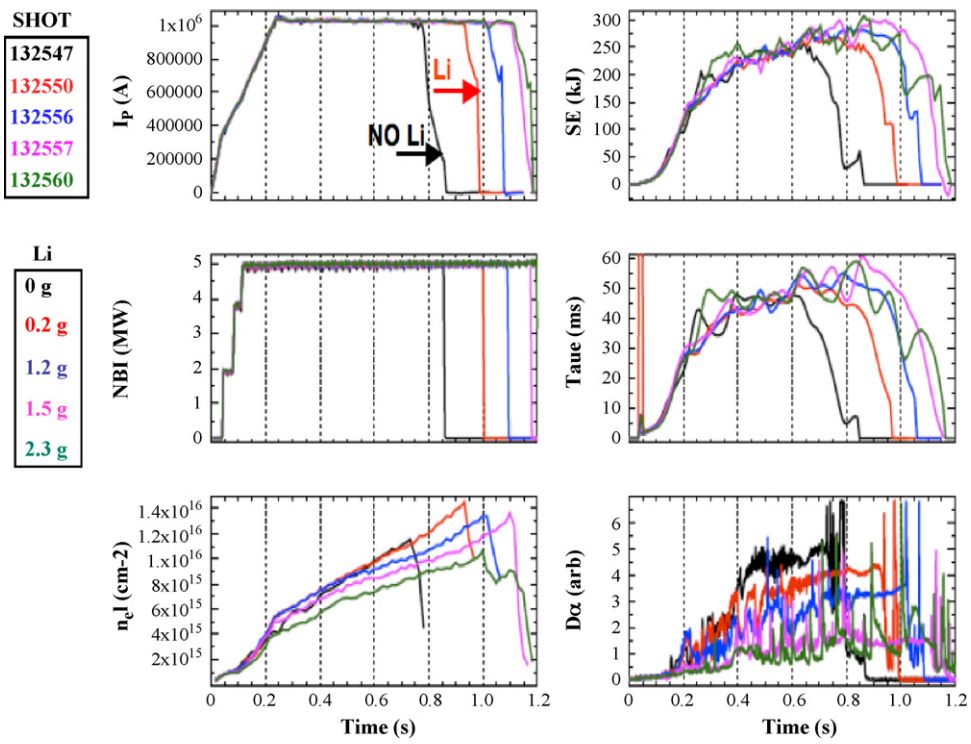

Fig. 2. Time evolution of representative plasma parameters for similar discharges without application of lithium and with increasing accumulation of lithium from LITERs.

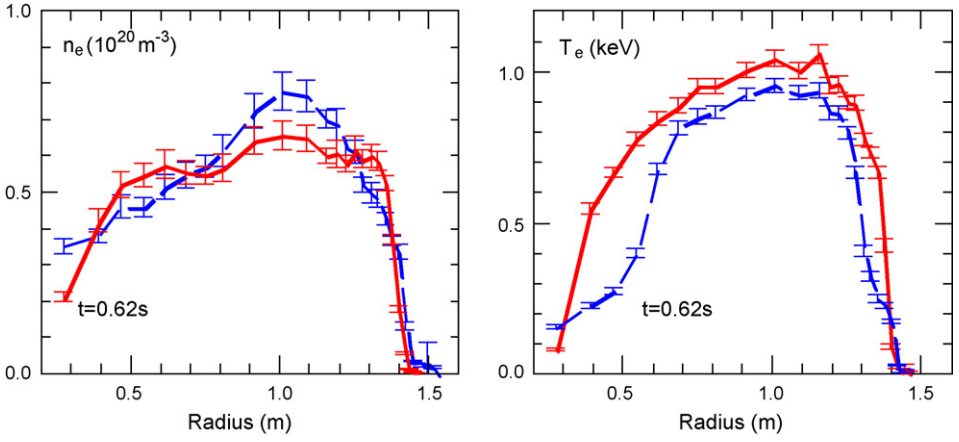

Fig. 3. Electron density and temperature profiles without lithium (blue) close to time of peak stored energy for plasma without lithium wall coating and discharge following evaporation of 250 mg of lithium (red).

absorbing and retaining hydrogen isotopes than lithium in its solid form. The LLD is located on the outer lower divertor plate, and at this location, predictions for its ability to provide significant edge pumping in NSTX will be tested.

4. LTX

The first construction phase of LTX has now been completed, and the machine achieved first plasma in 2008. Discharge development is underway, and installation of the remaining initial diagnostic set, as well as implementation of a novel insulated-gate bipolar transistor (IGBT)-based Ohmic power supply, which employs a transformer arrangement to permit independent switching of the individual paralleled IGBTs. Both elevation and cutaway CAD views of the tokamak are shown in Fig. 6, to illustrate the essential features of the device. The poloidal field coil set is visible in the external view of the device (Fig. 6(a)). The most prominent feature in the vacuum vessel is the heated shell, which will encase 90% of the last closed flux surface of the plasma. The field coils colored blue, red, yellow, and a new uncased internal coil comprise the poloidal field (PF) coil set for position control and shaping. All but the orange coils (which control vertical position and elongation) are new for LTX. Equilibrium calculations indicate that the new PF coil set will support discharges with plasma currents of over 400 kA, with a wide range of current profiles. Following full qualification of the power supplies, coils, and other components, lithium operation is expected to commence in early 2010.

5. Engineering of the LTX shell

Central to the LTX concept is the heated, conformal shell, which will be coated with molten lithium. The shell is formed of 1.5 mm thick 304 L stainless steel explosively bonded to 1 cm thick OFHC copper, and is heated with custom-length, commercial resistive

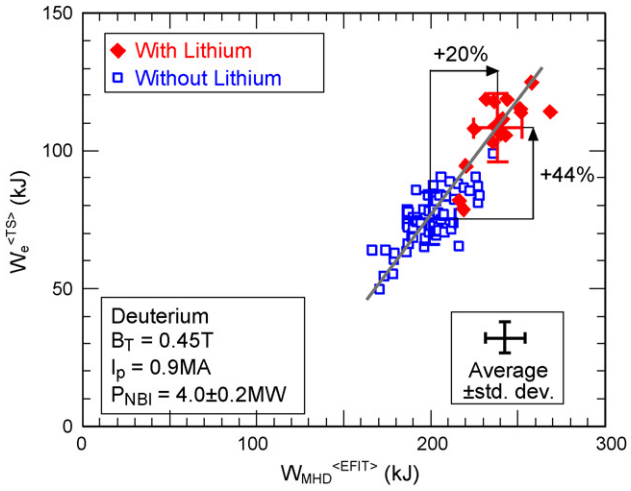

Fig. 4. Electron stored energy (W_e) as function of total stored energy (W_{MHD}) for similar discharges with and without lithium coating of lower vacuum vessel region. W_e is from volume integration of density and temperature data from Thomson scattering (TS) diagnostic, and W_{MHD} is from EFIT MHD equilibrium analysis.

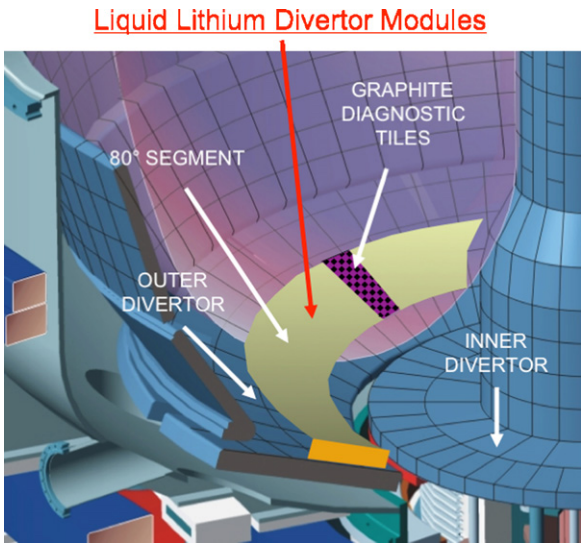

Fig. 5. Illustration of liquid lithium divertor (LLD) being installed in lower vacuum vessel of NSTX. Graphite tiles containing diagnostic sensors separate each of four LLD segments in outer divertor region.

cable heaters. The shell has two toroidal breaks and two poloidal breaks (the breaks in the shell are most clearly shown in Fig. 7). The outer equatorial plane break provides toroidally continuous diagnostic access, as well as an electrical break. The two toroidal breaks provide access for diagnostics such as Thomson scattering and the microwave interferometer system, which require good poloidal access. The shell is seen mounted in the vessel in Fig. 6(b).

The bonded stainless steel inner shell surface functions as a barrier to prevent attack of the copper by the liquid lithium. The copper backing is primarily designed to distribute heat and inhibit hot spot formation, either from the discrete electrical heaters or from plasma contact. Modeling [16] also indicates that the conducting shell, with a time constant of 140 ms, will have a significant effect on the plasma stability. Explosive bonding of the stainless to the copper backing was chosen only after several alternative electroplated and plasma-sprayed surfaces failed to protect the copper from attack by liquid lithium. Surfaces which failed include hard chromium plating over nickel, and plasma-sprayed tungsten and molybdenum. Thin electroplated nickel inhibits attack of the copper by liquid lithium, but only up to temperatures in the 400–500 °C range. The outer surface of the shell is plated with nickel, as are all other copper structures in the tokamak. A second shell is in fabrication, which will be plasma-sprayed with a 0.1–0.2 mm thick coating of porous molybdenum on the inner stainless steel surface. Porous molybdenum has been shown to retain thicker layers of lithium than can be achieved with thin films on stainless steel. Molybdenum of 30–60% porosity has been tested, and a porosity of approximately 50% has been chosen for the coating. Both the stainless steel inner surface for the first shell, and the molybdenum

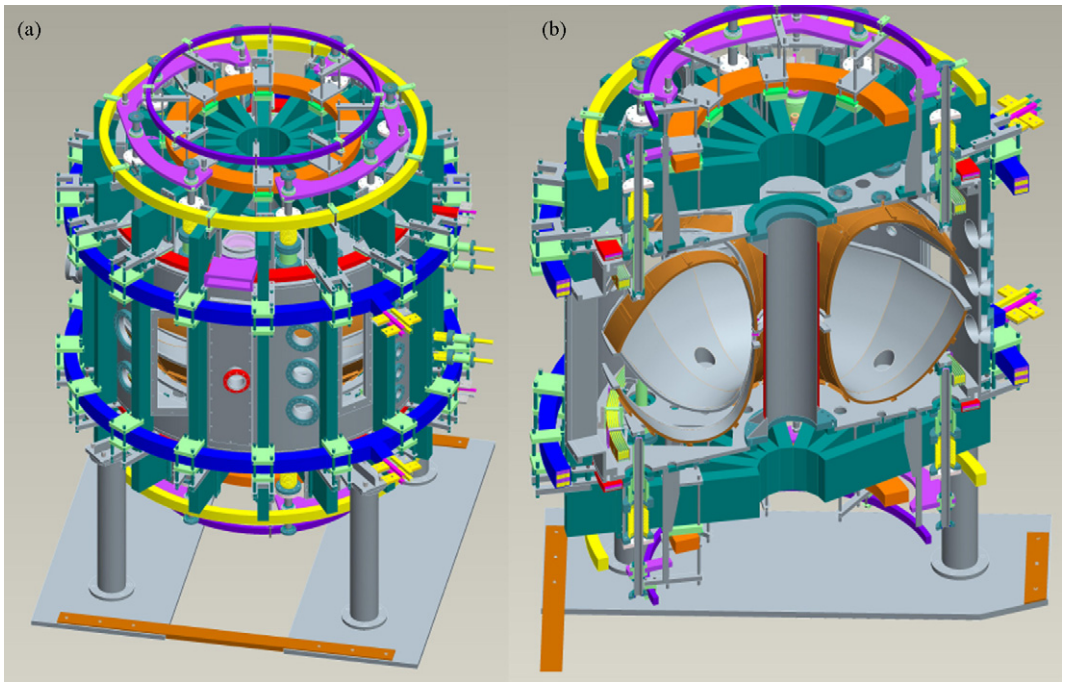

Fig. 6. Elevation (a) and section (b) of LTX, showing the internal heated shell.

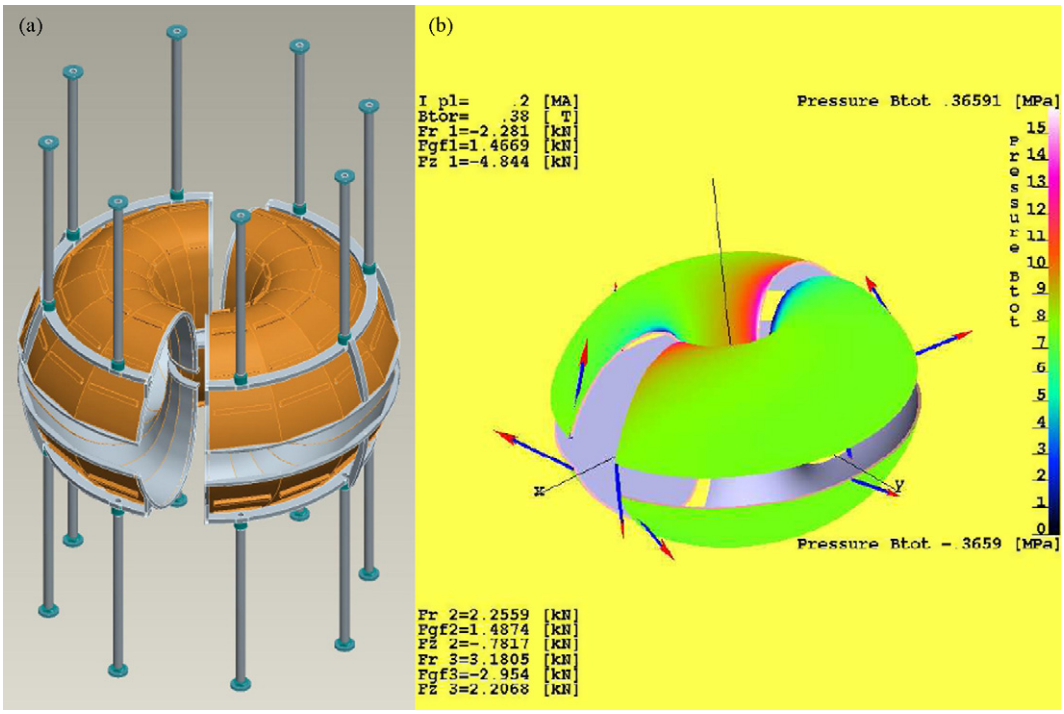

Fig. 7. CAD view of the shell and support structure (a), and calculated forces on the shell during a disruption (b). The total overturning moment on the shell is approximately 5 kN.

surface for the second shell, will be fully coated by lithium to inhibit sputtering of high-Z materials into the plasma.

Both views in Fig. 6 also show the shell support structure, which is designed for both mechanical and 1 kV electrical isolation of each of the four shell segments from the vacuum vessel. Mechanical support for the shell segments is provided by four legs per segment. Each leg extends through the upper and lower vessel flanges via a vacuum electrical break and a formed bellows, and is supported externally off the vacuum vessel. In effect, the shell "floats" within the vessel, with no internal electrical or mechanical contact between the shell and the vessel. This approach avoids supporting the shell segments on internal high voltage ceramic breaks, which would be subject to repeated mechanical shock during disruptions due to the overturning moment on the shell segments. The approach also allows for thermal expansion of the shell; expansion is accommodated by flexing of the long support legs. The shell itself, with support legs, is shown in Fig. 7(a), along with the calculated distribution of forces during a disruption, in Fig. 7(b). A photograph of the interior of the shell during a vent is shown in Fig. 8.

Resistive cable heaters (not shown) are clamped onto the outer, copper surface of the shell in order to maintain a temperature of up to 500–600 °C. These heaters are constructed with long cold sections at the terminating ends; all sections of the heater not in good thermal contact with the shell are unheated. Vacuum isolation is through Swagelok fittings sealed to the tubular heaters themselves, so that all electrical connections for the heaters are made outside the vessel, where they are not subject to coating by thin layers of evaporated lithium. The shell segments are individually electrically isolated through insulating supports and electrical breaks on the heater feedthroughs in order to facilitate argon glow-discharge cleaning of the inner shell surface. Heat conduction paths from the shell to the vacuum vessel are limited to the stainless steel support rings and legs (shown in Fig. 7(a)); these paths are over a meter long, and have small cross-sectional area to provide for good thermal isolation. The LTX centerstack is thermally isolated from the shell by a 1.5 mm layer of polished stainless steel, overlying a 1.5 mm layer of silicon bonded mica, and a 6 mm vacuum gap between the mica and the 1.5 mm thick Inconel tube, which comprises the vacuum boundary of the centerstack. The centerstack assembly contains the epoxy-potted Ohmic solenoid and inner toroidal field coil conductors, and is water-cooled. All coolant channels are segregated from lithium-coated areas by the vacuum boundary; only gas (helium) cooling is employed within the vacuum boundary. The vacuum chamber itself is externally water-cooled.

ANSYS analysis of the thermal performance of the shell and surrounding vacuum chamber indicates that operation to ~600 °C is feasible with the present 40 kW heater set, without additional provision for cooling. A plot of the temperature distribution over the shell, outer vacuum vessel, and centerstack is shown in Fig. 9, for 29 kW of heating power, with the shell temperature at 500 °C. Eight liters/minute of water flow, with a 30 °C temperature rise, is suf-

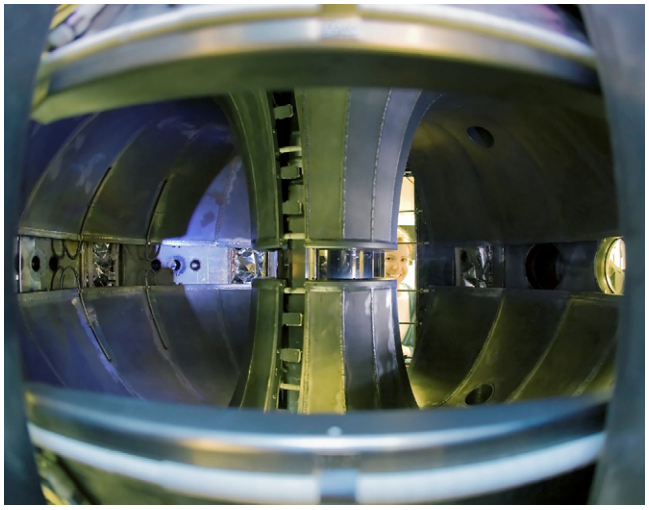

Fig. 8. Photograph of the interior of the LTX shell, during a recent vent. The vertical arrays of rectangular objects visible just left of center are the shields for the two-axis Mirnov coils in one of the shell gaps.

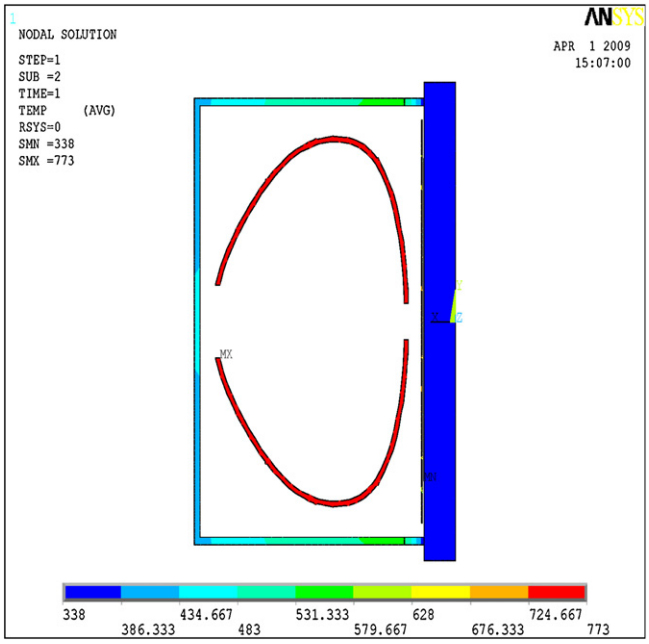

Fig. 9. Results of ANSYS thermal analysis of LTX with the internal shell at 500 °C, with 29 kW of shell heating power.

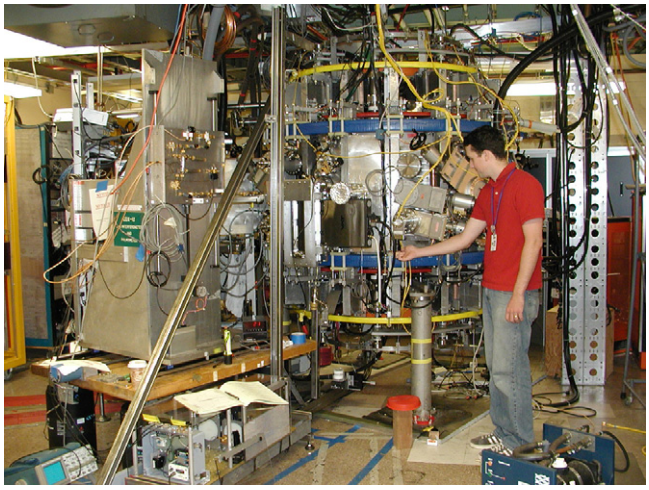

Fig. 10. Photograph of LTX shortly following pumpdown after the 2009 vent.

ficient to cool the outer vacuum vessel. The centerstack remains below 40 °C, well below the temperature limit for the centerstack of 85 °C.

Recently, the shell heating and vessel cooling systems were tested to a shell temperature of 200 °C, above the melting point of lithium. During this test, the temperatures of all sections of all four shell segments were easily held to within 5 °C, without elaborate temperature control. The temperature rise of the outer Inconel surface of the centerstack was just 2 °C, while the vacuum vessel (with air cooling only, as water flow was not required) remained below 50 °C.

A recent photograph of the assembled LTX is shown in Fig. 10.

6. Engineering LTX for liquid lithium

We have already noted that extensive testing was required to qualify a suitable substrate for liquid lithium, in order to construct the LTX heated shell. In fact, although pure, solid, room temperature lithium does not attack materials commonly used in fusion experiments, liquid lithium (melting point 180.5 °C) does. Copper, gold, platinum, aluminum, aluminum oxide, and many other materials used in fusion experiments are not suitable for use in contact with liquid lithium [17]. Nickel and alloys (e.g. Inconel) can be used up to 400–500 °C, although Inconel has inferior resistance to lithium when compared to steels. Austenitic and especially ferritic stainless steels can be employed to temperatures in excess of 600 °C. The refractory metals (tungsten, molybdenum, vanadium, scandium, tantalum) all have good tolerance to liquid lithium at elevated temperatures. However, carbon is well-known to be incompatible with liquid lithium at any temperature above the melting point. Only one ceramic (yttria) has been identified which will tolerate contact with liquid lithium at temperatures in excess of 400 °C. We have conducted successful short-term (~1 h) tests of lithium-filled yttria crucibles to 600 °C with no sign of attack. Boron nitride and yttria-stabilized magnesium oxide have use temperatures extending to approximately 400 °C, however. Winding forms for the Mirnov coils in LTX have been machined from yttria-stabilized MgO. Quartz can tolerate liquid lithium up to 300–350 °C; fiberglass insulation is usable to temperatures of approximately 350 °C.

As a result, many materials which are commonly utilized in fusion experiments have been excluded from LTX. In cases where materials which are not tolerant to liquid lithium must be used – for example, in the many vacuum electrical breaks employed for electrical isolation – the few alumina insulators in LTX must be shielded from lithium vapor.

In CDX-U, reduced optical transmission through vacuum windows due to lithium coatings was a serious issue. On LTX, all windows, without exception, are gate-valve mounted to permit removal and cleaning of the window. Sensitive windows, such as the Thomson scattering viewing window, are equipped with automatic shutters, in addition to being gate-valve mounted.

7. Projected performance of LTX

Results from NSTX cited in this paper, and earlier results from CDX-U [7,18], indicate that confinement is strongly enhanced with lithium PFCs. In particular, the results from CDX-U provided strong correlation between enhanced confinement and a reduction in recycling to the ~60% level [7]. A model has been developed for the performance of discharges in LTX with further reductions in the global recycling coefficient provided by full liquid lithium walls [18]. Modeling indicates that the effects of low recycling walls on confinement should be significant, even in Ohmic operation [18]. Modest neutral beam heating in LTX should achieve plasma temperatures in the 1–2 keV range. Neutral beam heating will be available on LTX in the 2011 time frame, with a 5 A, 20 keV hydrogen beam.

Acknowledgment

This work was supported by US DOE contract DE-AC02-09CH11466.

References

[1] M. Ono, et al., Nucl. Fusion 40 (2000) 557–561.
[2] M.G. Bell, et al., Nucl. Fusion 46 (2006) S565–S572.
[3] D.K. Mansfield, et al., Nucl. Fusion 41 (2001) 1823–1834.
[4] S.V. Mirnov, V.B. Lazarev, S.M. Sotnikov, V.A. Evtikhin, I.E. Lyublinski, A.V. Vertkov, Fusion Eng. Des. 65 (2003) 455–465.
[5] M.L. Apicella, et al., J. Nucl. Mater. 363–365 (2007) 1346–1351.
[6] J. Sanchez, et al., J. Nucl. Mater. 390–391 (2009) 852–857.
[7] R. Majeski, et al., Phys. Rev. Lett. 97 (2006) 075002.
[8] R. Kaita, et al., Phys. Plasmas 14 (2007) 056111.

[9] H.W. Kugel, et al., J. Nucl. Mater. 363–365 (2007) 791–796.
[10] H.W. Kugel, et al., J. Nucl. Mater. 337–339 (2005) 495–499.
[11] H.W. Kugel, et al., Phys. Plasmas 15 (2008) 056118.
[12] D.K. Mansfield, et al., J. Nucl. Mater. 390–391 (2009) 764–767.
[13] R. Maingi, et al., Phys. Rev. Lett. 103 (2009) 075001.
[14] S.A. Sabbagh, et al., Nucl. Fusion 41 (2001) 1601–1611.
[15] M.G. Bell, et al., Plasma Phys. Control. Fusion 51 (2009) 124054 (12pp).
[16] J. Manickam, et al., MHD stability limits in the Lithium Tokamak eXperiment (LTX), Bull. Am. Phys. Soc. (2008), http://meetings.aps.org/link/BAPS.2008.DPP.NP6.133.
[17] D.W. Jeppson, J.L. Ballif, W.W. Yuan, B.E. Chou, Lithium Literature Review: Lithium's Properties and Interactions, Hanford Engineering Development Laboratory publication HEDL-TME 78-15 UC-20, 1978, April.
[18] R. Majeski, et al., Nucl. Fusion 49 (2009) 055014.